Effect of Reagent Rotation on Isotopic Branching in (He, HD^+) Collisions

Ashwani Kumar Tiwari and N. Sathyamurthy*

Department of Chemistry, Indian Institute of Technology Kanpur, Kanpur 208016, India

Received: June 5, 2006; In Final Form: July 20, 2006

A three-dimensional time-dependent quantum mechanical wave packet approach is used to calculate reaction probability (P^R) and integral reaction cross section (σ^R) values for both the channels of the reaction He + HD^+ (v = 1; j = 0, 1, 2, 3) → HeH(D)$^+$ + D(H), over a range of translational energy (E_{trans}) on the McLaughlin−Thompson−Joseph−Sathyamurthy (MTJS) potential energy surface using centrifugal sudden approximation for nonzero total angular momentum (J) values. The reaction probability plots as a function of translational energy for different J values exhibit several oscillations, which are characteristic of the system. It is shown that HeH^+ is preferred over HeD^+ for large J values and that HeD^+ is preferred over HeH^+ for small J values for all the rotational (j) states studied. The integral reaction cross section for both the channels and therefore the isotopic branching ratio for the reaction depend strongly on j in contrast to the marginal dependence shown by earlier QCT calculations. The computed results are in overall agreement with the available experimental results.

I. Introduction

The dynamics of (He, H_2^+) collisions has been studied extensively over the years due to its importance in interstellar medium and plasmas.[1,2] Yet, our understanding of this ion−molecule system is not complete. There are several aspects of the dynamics that remain to be accounted for quantitatively. In the isotopomeric reaction He + HD^+, the helium atom can attack at either end of HD^+, leading to two different products

$$\mathrm{He} + \mathrm{HD}^+ \rightarrow \mathrm{HeH}^+ + \mathrm{D} \qquad \text{(R1a)}$$

$$\rightarrow \mathrm{HeD}^+ + \mathrm{H} \qquad \text{(R1b)}$$

Despite its simplicity and fundamental importance, experimental studies on reactions (R1a) and (R1b) have been limited. Klein and Friedman[3] measured the isotopic branching ratio [$\Gamma_\sigma = \sigma^R(HeH^+)/\sigma^R(HeD^+)$] in (He, HD^+) collisions. They reported that Γ_σ increased with an increase in relative translational energy (E_{trans}), reached a maximum, and then started decreasing with an increase in energy. The value of Γ_σ remained less than unity over the entire range of E_{trans} (0−8.0 eV). Turner et al.[4] measured initial vibrational (v) state resolved integral reaction cross section values and reported vibrational enhancement for both the channels up to E_{trans} = 4.0 eV. Γ_σ remained less than unity over the entire collision energy range (1.0−8.0 eV) for v = 0 and 1. For v = 2 also, Γ_σ was less than unity for all translational energy values reported except for E_{trans} = 1.0 eV, when it was 1.04.

Using a three-dimensional (3D) quasiclassical trajectory (QCT) method, Bhalla and Sathyamurthy[5] computed σ^R values for both the channels of the reaction for v = 0−4 and j = 0 of HD^+ on a McLaughlin−Thompson−Joseph−Sathyamurthy (MTJS) potential energy surface (PES).[6] They reproduced the vibrational enhancement of the reaction cross section in near quantitative agreement with experiment. However, the branching ratio obtained by their calculations was only half of what was reported from experiments[4] for v = 4 of HD^+ at E_{trans} = 1.0 eV. Kumar et al.[7] computed rotationally resolved σ^R values using the 3D QCT method and found that it was independent of j. Therefore, they concluded that discrepancies between theory and experiment could arise either due to the fact that the QCT method was not good enough to incorporate the quantum effects that could be present in the system or the PES was not accurate enough.

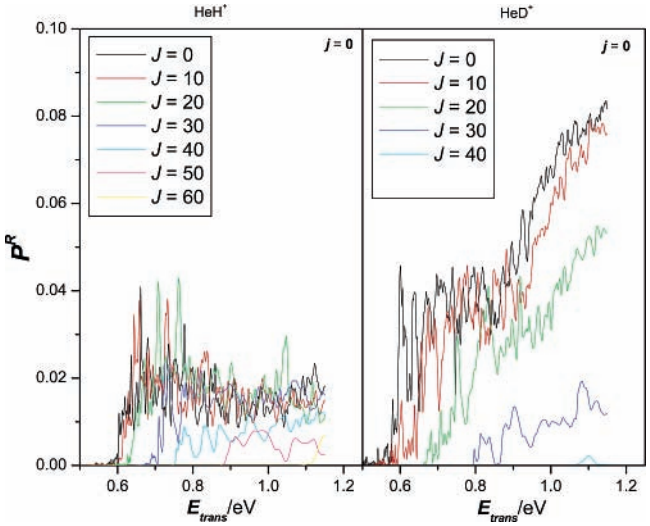

Figure 1. Plot of reaction probability values as a function E_{trans} for j = 0 of HD^+.

Kalyanaraman et al.[8] carried out 3D time-dependent quantum mechanical (TDQM) wave packet calculations and computed j-resolved reaction probability (P^R) values for both channels of the reaction on the MTJS PES for total angular momentum J = 0 and found that P^R and therefore Γ_P [= $P^R(HeH^+)/P^R(HeD^+)$] was highly dependent on j. However, it was not clear if the j-dependence of Γ_P would survive J averaging. The issue could not be settled because of limited computational resources available at that time. Recently, Tiwari et al.[9] computed integral reaction cross section values for reactions (R1a) and (R1b) for

* To whom correspondence should be addressed. E-mail: nsath@iitk.ac.in.

10.1021/jp063470+ CCC: $33.50
Published on Web 09/06/2006

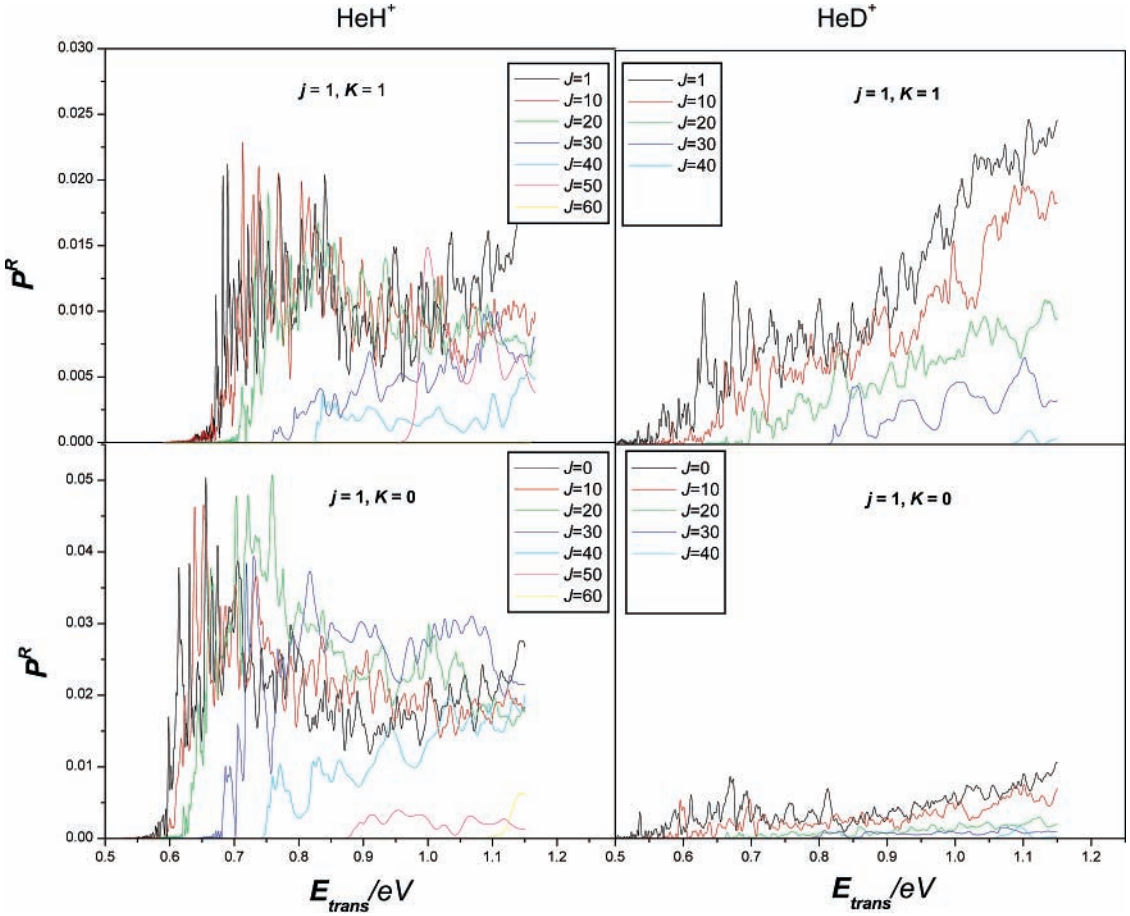

Figure 2. Same as that for Figure 1 for $j = 1$ of HD^+.

$v = 0-3$, $j = 0$ of HD^+ on the MTJS and the recently published Palmieri et al.[10] potential energy surfaces. The results were nearly the same on both the potential energy surfaces. Therefore, to see if the j-dependence of Γ_P would survive J averaging, a detailed J-converged 3D TDQM study of the reaction for $v = 1$ and $j = 0-3$ of HD^+ on the MTJS PES was undertaken. Details of the methodology are given in section II, and the results are presented and discussed in section III. Summary and conclusion follow in section IV.

II. Methodology

The TDQM methodology[11,12] used involves solving the time-dependent Schrödinger equation in reactant channel Jacobi coordinates on a three-dimensional grid. For a triatomic system, the Hamiltonian operator in (R,r,γ) space is given as[13]

$$\mathbf{H} = -\frac{\hbar^2}{2\mu_R}\frac{\partial^2}{\partial R^2} - \frac{\hbar^2}{2\mu_r}\frac{\partial^2}{\partial r^2} + \frac{(\mathbf{J}-\mathbf{j})^2}{2\mu_R R^2} + \frac{\mathbf{j}^2}{2\mu_r r^2} + V(R,r,\gamma) \quad (1)$$

where μ_R is the reduced mass of He with respect to the center-of-mass of HD^+ and μ_r is the reduced mass of HD^+. R is the center-of-mass separation between He and HD^+, r is the separation between H and D, and γ is the angle between R and r. **J** is the total angular momentum operator and **j** the rotational angular momentum operator for the diatomic species. $V(R,r,\gamma)$ is the interaction potential.

The initial wave packet for the time evolution was chosen as

$$\psi(R,r,\gamma,t=0) = G_{k0}(R)\phi_{vj}(r)P_{jK}(\cos\gamma) \quad (2)$$

TABLE 1: Grid Parameters and Initial Condition Details for $J \leq 13$ (see text for $J > 13$)

parameters	values	descriptions
N_R	128	number of grid points in R
$(R_{min}, R_{max})/a_0$	(1.50, 16.74)	range of R values
N_r	80	number of grid points in r
$(r_{min}, r_{max})/a_0$	(1.00, 12.06)	range of r values
N_γ	54	number of grid points in γ
Δt/fs	0.2419	time step used in propagation
T/ps	1.2	propagation time
R_0/a_0	12.0	center of initial wave packet
δ/a_0	0.25	Gaussian width parameter
r_s/a_0	7.0	position of the analysis surface

where

$$G_{k0} = \left(\frac{1}{\pi\delta^2}\right)^{1/4} \exp\{-(R-R_0)^2/2\delta^2\} \exp(-ik_0R) \quad (3)$$

with R_0 and k_0 referring to the center of the wave packet in position and momentum space, respectively. δ is the width parameter for the wave packet, K is the projection of J on the body fixed z axis (taken along R), and $P_{jK}(\cos\gamma)$ represents the associated Legendre polynomials.

The diatomic rovibrational eigenfunctions $\phi_{vj}(r)$ for HD^+ were computed by means of the Fourier grid Hamiltonian approach.[14]

The split-operator method[15] was used to propagate the wave packet in time. The fast Fourier transform (FFT) method[16] was used to solve the radial part of the Schrödinger equation, and the discrete variable representation (DVR)[17] was used for the angular part. The time-dependent Schrödinger equation was solved under centrifugal sudden approximation,[18] and the wave

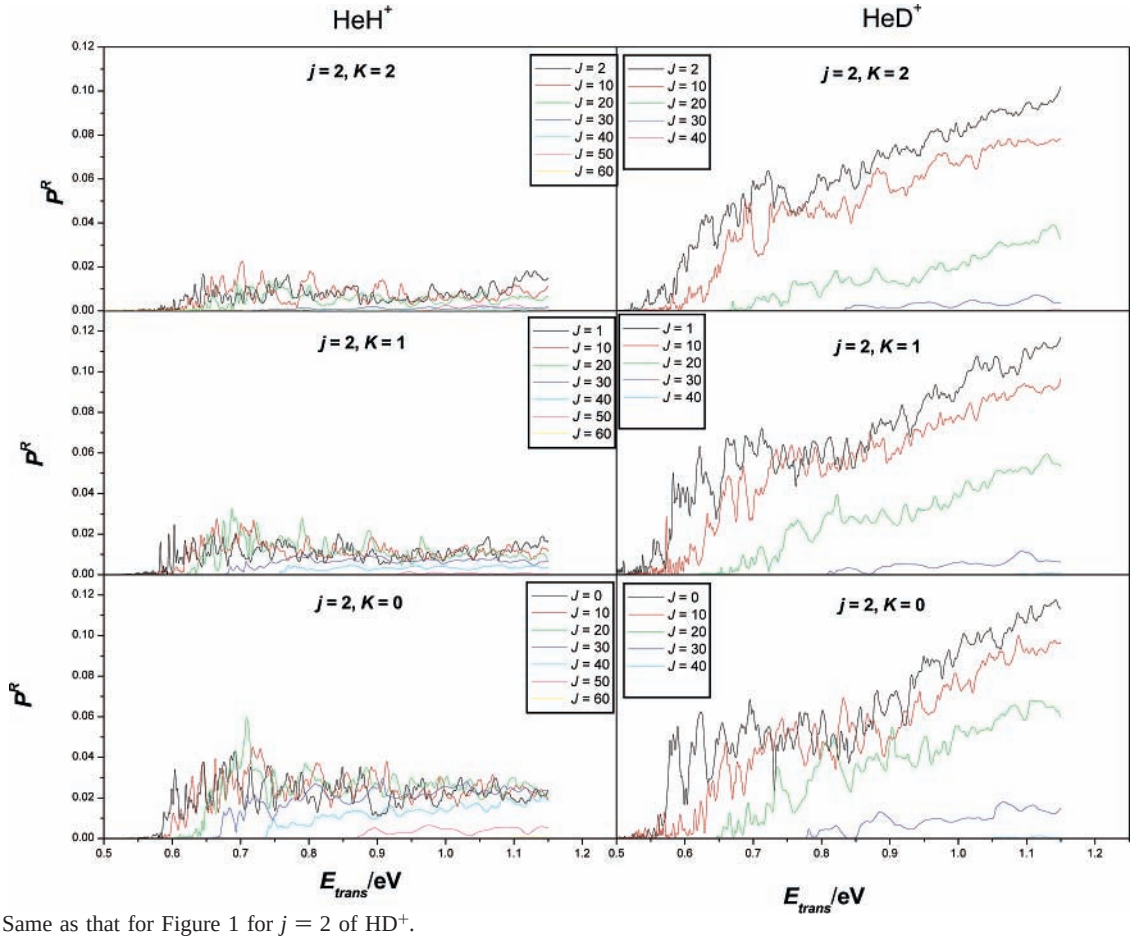

Figure 3. Same as that for Figure 1 for $j = 2$ of HD^+.

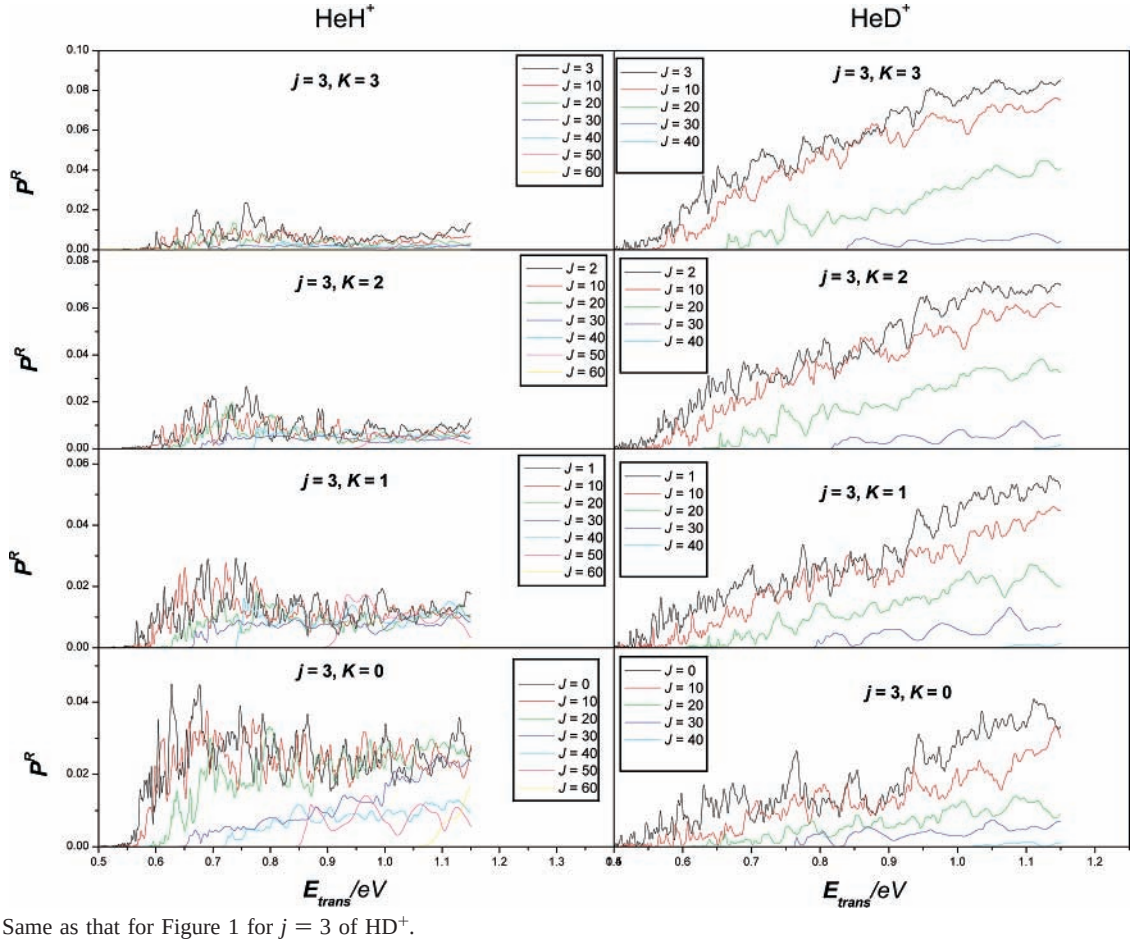

Figure 4. Same as that for Figure 1 for $j = 3$ of HD^+.

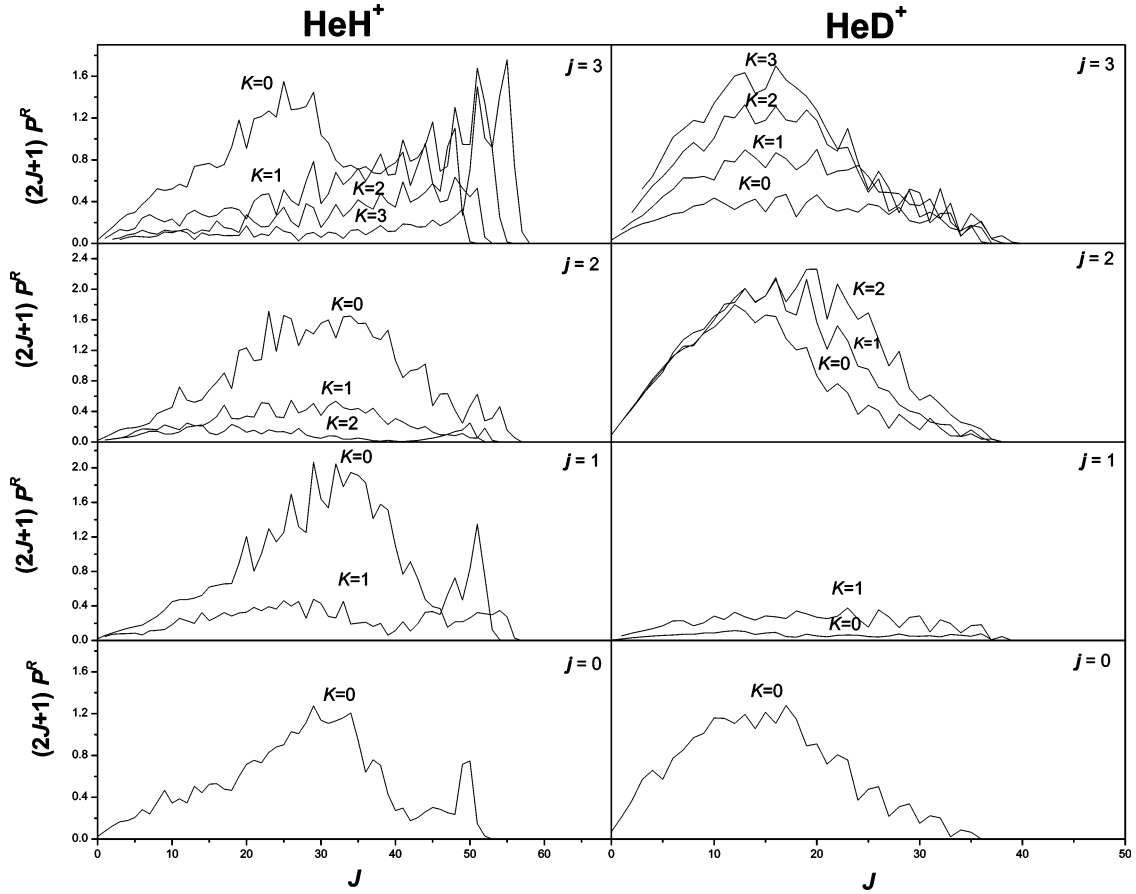

Figure 5. Plot of partial reaction cross section values as a function of J, comparing the contribution from different K values to the cross section for HeH^+ and HeD^+ at $E_{trans} = 1.0$ eV.

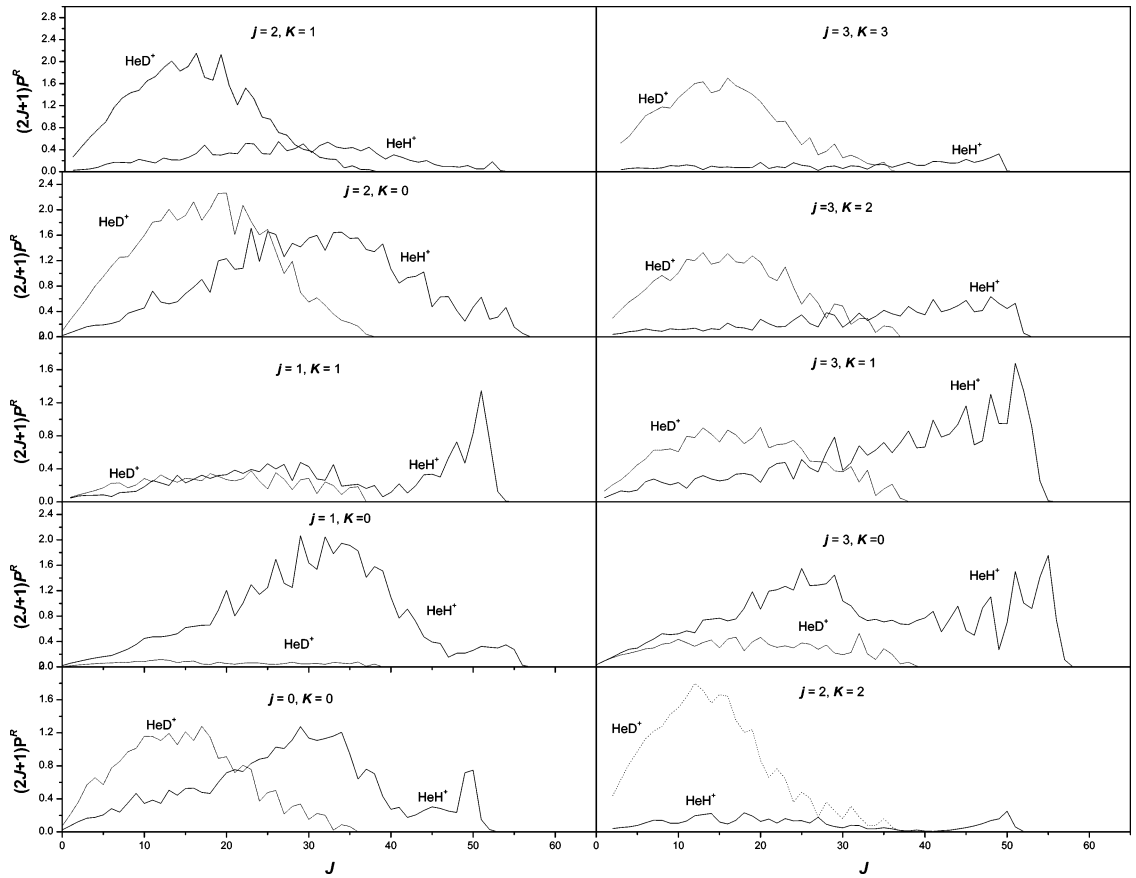

Figure 6. Comparison of partial reaction cross section values as a function of J for HeH^+ and HeD^+ formation for different j and K values at $E_{trans} = 1.0$ eV.

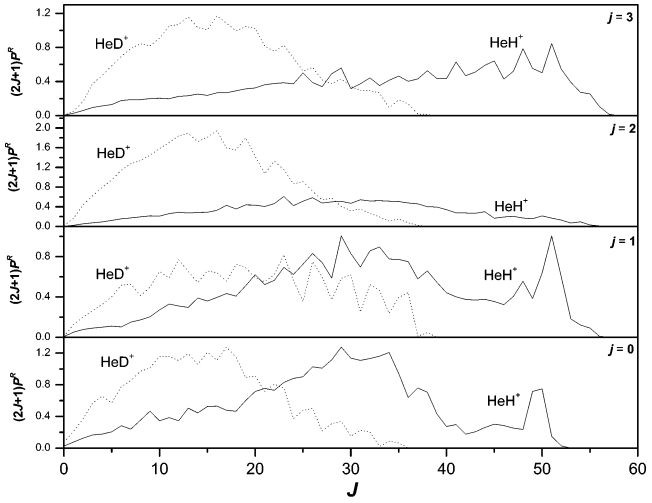

Figure 7. Plot of *K*-weighted partial cross section values as a function of J at $E_{trans} = 1.0$ eV.

packet was propagated for 1.20−1.70 ps. Having computed $\psi(R,r,\gamma,t)$ at time t, the energy-resolved reaction probability $P_{vj}^{JK}(E)$ was calculated as[7]

$$P_{vj}^{JK}(E) = \frac{\hbar}{\mu_r} Im\left[\int_0^\infty dR \int_0^\pi d\gamma \sin\gamma \psi^*(R,r,\gamma,E) \frac{d}{dr} \psi(R,r,\gamma,E)\right]_{r=rs} \quad (4)$$

where the energy-dependent wave function $\psi(R,r,\gamma,E)$was obtained by Fourier transforming the time-dependent wave packet $\psi(R,r,\gamma,t)$.

Distance criteria have been used to assign the flux to each channel. If r_{HeH^+} is less than r_{HeD^+}, then the flux is assigned to the HeH^+ channel. Otherwise, it is assigned to HeD^+. For computing reaction probabilities corresponding to the HeH^+ and HeD^+ channels, r_s has been taken to be sufficiently large and away from the interaction region. Depending upon the values of r_{HeH^+} and r_{HeD^+}, the flux was integrated into either of the two channels. It was verified that the sum of the reaction probabilities obtained from individual product channels and the total reaction probability obtained directly from the energy-resolved flux out of the reactant channel were equal.

The J-dependent initial state-selected partial reaction cross section σ_{vj}^J was determined as

$$\sigma_{vj}^J(E) = \frac{1}{(2j+1)} [P_{vj}^{JK=0}(E) + 2\sum_{K=1}^{j} P_{vj}^{JK}(E)] \quad (5)$$

The initial state-selected total reaction cross section $\sigma_{vj}(E)$ was then obtained by summing over the partial reaction cross section values for all the partial waves

$$\sigma_{vj}(E) = \frac{\pi}{k_{vj}^2} \sum_{J=0}^{J_{max}} (2J+1)\sigma_{vj}^J(E) \quad (6)$$

The parameters used in the calculations up to $J = 13$ are given in Table 1. For $J > 13$, R_0 was increased by one atomic unit for each unit increase in J. Correspondingly, the time duration of propagation of the wave packet is also increased. Further details of the methodology can be seen in our earlier publication.[19]

III. Results and Discussion

A. Reaction Probabilities and Partial Reaction Cross Sections. Computed P^R values for both the product channels

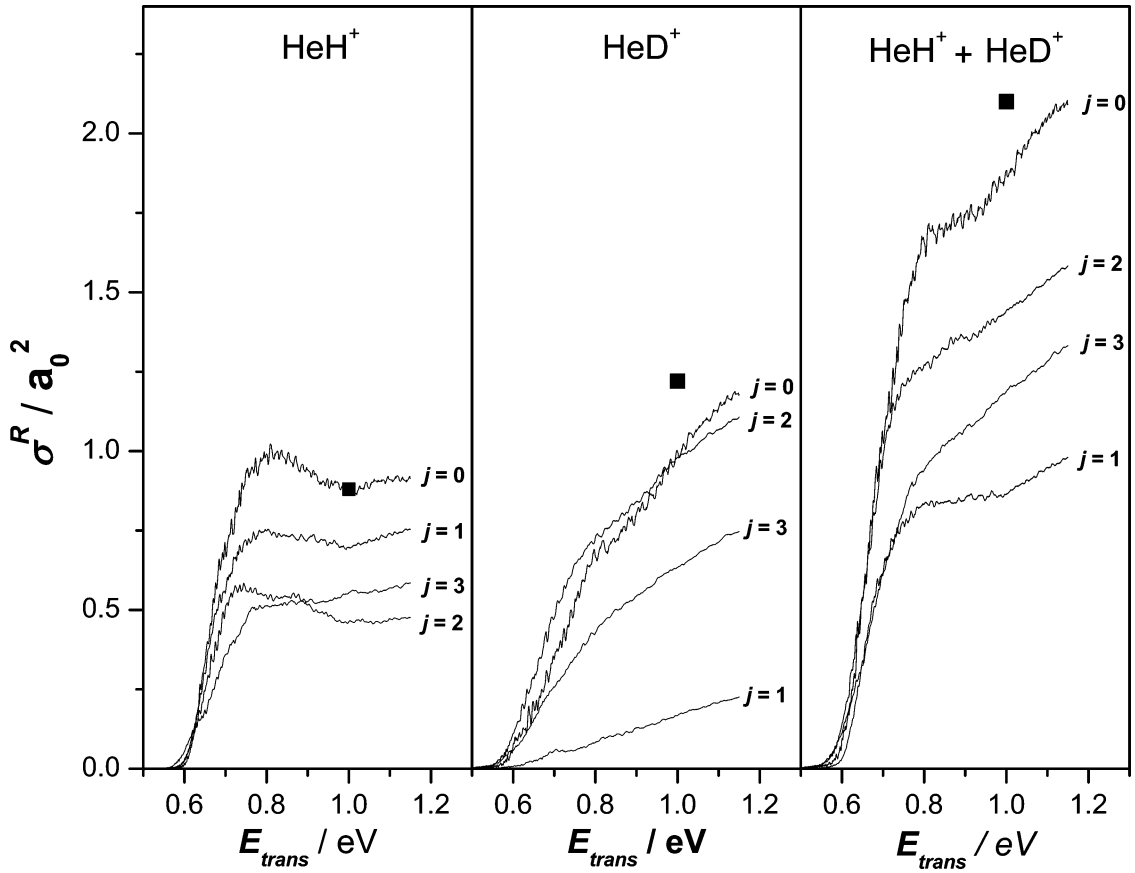

Figure 8. Plot of the integral reaction cross section as a function of E_{trans} along with the experimental values at $E_{trans} = 1.0$ eV, for both channels.

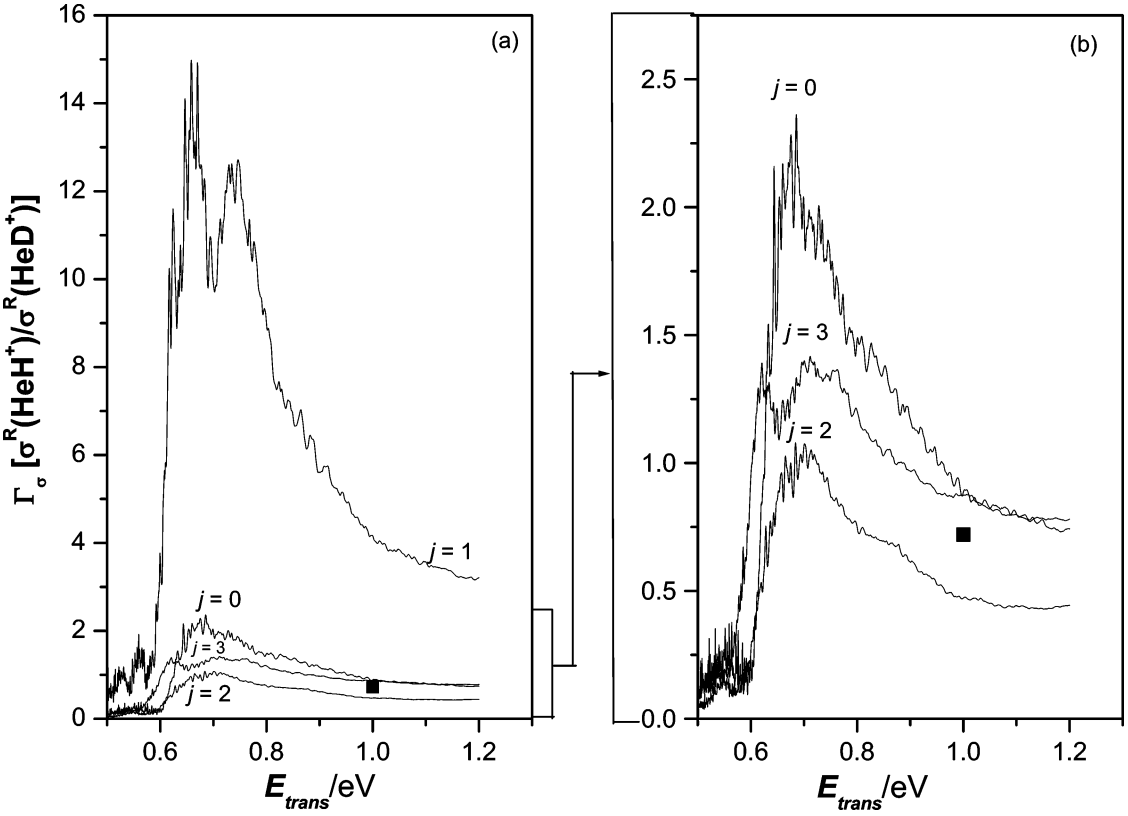

Figure 9. (a) Plot of the isotopic branching ratio as a function of E_{trans} along with the experimental value at $E_{trans} = 1.0$ eV for $j = 0-3$. The blown up plot for $j = 0$, 2, and 3 is shown in panel (b).

are plotted as a function of E_{trans} for a range of J values for $j = 0$, 1, 2, and 3 of HD^+ in Figures 1, 2, 3, and 4, respectively. Clearly, there are large number of oscillations in $P^R(E_{trans})$, particularly for the lower values of J, indicating the importance of reactive scattering resonances in (He, HD^+) dynamics. For $j = 0$, there is an overall increase in P^R for HeD^+ with an increase in E_{trans}. For the HeH^+ channel, on the other hand, P^R reaches a maximum and then it levels off about a mean line (not shown). Further, with an increase in J, the P^R values for HeD^+ formation decline more rapidly than the P^R values for HeH^+.

For $j = 1$, there are two possible initial values of helicity quantum number K: 0 and 1. For $K = 0$, the P^R values for HeH^+ formation are significantly larger than that for HeD^+ for all values of J over the entire energy range. The $P^R(E_{trans})$ plots for $j = 1$, $K = 1$, are similar to those for $j = 0$. For $j = 2$, the P^R values for the HeH^+ channel are lower than the P^R values for HeD^+ for all helicity quantum numbers ($K = 0$, 1, and 2). Also, there is an overall increase in P^R values for the HeD^+ channel with an increase in E_{trans} (for all the K values). For the HeH^+ channel, despite the oscillations, the P^R values change only marginally with an increase in E_{trans}. For $j = 3$, $K = 0$, the P^R values for HeH^+ formation are larger than that for HeD^+ over the entire E_{trans} range. For $K = 1$, the P^R values for HeH^+ are larger than those for HeD^+ at low energies. At higher energies, HeD^+ is preferred over HeH^+. For $K = 2$ and 3, HeD^+ is preferred over HeH^+ over the entire E_{trans} range. It is worth pointing out that the P^R values for HeD^+ formation become zero by the time J becomes 40. However, for HeH^+, calculations had to be carried for values up to $J = 60$ for all j and K values under investigation.

The role of K on the computed reaction cross section becomes evident from the plots of the partial cross section $[(2J + 1)P^R]$ as a function of J for different values of j and K for $E_{trans} = 1.0$ eV in Figure 5. Clearly, the formation of HeH^+ decreases with an increase in K, whereas formation of HeD^+ increases with an increase in K. For a given j, $K = 0$ represents the physical situation, in which HD^+ is rotating in the triatomic plane containing the relative velocity vector. $K = j$, on the other hand, corresponds to the situation in which the plane of rotation of HD^+ is perpendicular to the plane of orbital motion of He with respect to HD^+. The intermediate values of K represent the intermediate angles between the two planes. In the simplest model, one understands that the center of mass of HD^+ is shifted toward the D atom, and in rotating HD^+, the H atom sweeps a larger area than the D atom. Therefore, the approaching helium atom has more access to the H atom for abstraction and HeH^+ is the preferred product. This model is perfectly alright for $K = 0$, corresponding to the planar (He, HD^+) dynamics. But for $K > 0$, where orbital motion and rotational motion are not coplanar, the possibility of He attacking at the intermediate regions between H and D ends increases and therefore the possibility of formation of $[H\cdots He\cdots D]^+$ increases. This would invariably result in the formation of HeD^+ because of the ease of ejection of the lighter H atom. These two competing pathways would account for the difference in the dependence of partial cross section on K. Further, our results suggest that with increasing K, the complex forming mechanism becomes the predominant pathway.

To examine the preferential formation of one isotopomer over another as a function of J, the partial cross section $[(2J + 1)P^R]$ for both the channels at $E_{trans} = 1.0$ eV are plotted for $v = 1$, $j = 0$, 1, 2, and 3 in Figure 6. For $j = 0$, $K = 0$, $j = 2$, $K = 0$, 1, and for $j = 3$, $K = 1-3$, HeD^+ is preferred over HeH^+ at low J values, whereas the trend gets reversed for high J values. For $j = 1$, $K = 0$ and $j = 3$, $K = 0$, HeH^+ is preferred over

HeD^+ for all J values, whereas for $j = 2$, $K = 2$, HeD^+ is preferred over HeH^+ for all J values. For $j = 1$, $K = 1$, HeD^+ is preferred over HeH^+ up to only $J = 10$, and for higher values of J, HeH^+ is preferred. In a recent publication[9] using the TDQM method, it was shown that HeH^+ was preferred over HeD^+ at high J values and HeD^+ was preferred at low J values for $v = 1$, 2, and 3, $j = 0$ of HD^+. Since $J \propto b$ (impact parameter) and b is related to scattering angle, it was inferred that HeH^+ would be preferred over HeD^+ in the forward direction, while HeD^+ would be preferred over HeH^+ in the backward direction. For $v = 0$, HeH^+ was preferred over HeD^+ for all J values and hence was expected to be preferred in all directions. This inference was verified by computing differential cross section using the time-independent quantum mechanical (TIQM) method.[20] By the same logic, it can be concluded that HeH^+ would be preferred over HeD^+ in the forward direction and HeD^+ would be preferred over HeH^+ in the backward direction for $j = 0$, $K = 0$; $j = 2$, $K = 0$ and 1; $j = 3$, $K = 1-3$. For $j = 1$, $K = 0$ and $j = 3$, $K = 0$, HeH^+ would be preferred in all directions, whereas HeD^+ would be preferred over HeH^+ in all directions for $j = 2$, $K = 2$. Since K is not amenable to experiment, one should really compare the K averaged partial cross section values for the two channels to predict the preferential scattering of isotopomers. The same is plotted in Figure 7. Clearly, the partial cross section for HeD^+ is larger than that for HeH^+ at low J values for all j. For higher J values, the trend is reversed for all j. Therefore, HeH^+ would be preferred over HeD^+ in the forward hemisphere, while HeD^+ would be preferred over HeH^+ in the backward hemisphere for all j states for which the dynamics has been investigated. A similar conclusion was arrived at by Kumar et al. based on QCT calculations.[6]

B. Reaction Cross Section and Isotopic Branching Ratios. After computing the reaction probability values until convergence with respect to J, the integral reaction cross section values for the formation of HeH^+ and HeD^+ were calculated for $v = 1$, $j = 0$, 1, 2, and 3. The results are plotted as a function of E_{trans} in Figure 8 for both the channels, along with the experimental values for $v = 1$ at $E_{trans} = 1.0$ eV.[4] It is clear that the σ^R values depend significantly on j in contrast to the marginal dependence reported by earlier QCT calculations.[6] The discrepancy between the TDQM and QCT results could arise from the quantum mechanical resonances present in the system. Aquilanti et al.[21] have carried out a detailed analysis of the quantum effects by examining the dynamics in three dimensions on three different PESs. For the HeH^+ channel, σ^R increases with an increase in E_{trans}, reaches a maximum, and then nearly becomes independent of E_{trans} for all rotational states. On the other hand, for the HeD^+ channel, it increases continuously with an increase in E_{trans}. Further, the integral reaction cross section for HeH^+ formation decreases in going from $j = 0$ to 3 at lower energies. At ~0.9 eV, there is a crossing between the excitation function plots for $j = 2$ and $j = 3$. For HeD^+, the j-dependence is unusual. The $\sigma^R(E_{trans})$ value declines dramatically in going from $j = 0$ to $j = 1$ and then it increases and becomes nearly equal to the result for $j = 0$, when j changes from 1 to 2. Upon further increase in j to 3, there is a substantial decrease in cross section values. The total ($HeH^+ + HeD^+$) integral cross section follows the trend $j = 0 > j = 2 > j = 3 > j = 1$ over the entire E_{trans} range. The TDQM results are compared with the available experimental results for $v = 1$ at $E_{trans} = 1.0$ eV. It is clear that the experimental σ^R value for the formation of HeH^+ lies exactly on the $j = 0$ plot. For the HeD^+ channel, the experimental value is slightly larger than that computed for $j = 0$ and therefore the total experimental integral reaction cross section is also slightly larger than that computed for $j = 0$. Unfortunately, experimental results for initial j-state resolved reaction cross section values are not available for the system until this date.

The isotopic branching ratio Γ_σ is plotted as a function of E_{trans} for different j values in Figure 9. It is clear that, for all rotational states, Γ_σ increases with an increase in E_{trans}, reaches a maximum, and then starts decreasing with an increase in E_{trans}. The Γ_σ values for $j = 1$ are the largest and are smallest for $j = 2$. Further, for $j = 1$, HeH^+ is highly preferred over HeD^+ over the entire translational energy range except for 0.5 eV $\leq E_{trans} \leq$ 0.6 eV. For $j = 2$, Γ_σ is less than unity over the entire E_{trans} range. For $j = 0$ and 3, Γ_σ is less than unity below ~0.6 eV and above ~0.9 eV. The only available experimental value for Γ_σ lies slightly below the theoretical results for $j = 0$ and 3.

IV. Summary and Conclusions

Initial state-selected reaction probabilities and integral reaction cross section values for reactions (R1a) and (R1b) have been computed using a time-dependent quantum mechanical wave packet approach on an MTJS potential energy surface, within the centrifugal sudden approximation. It is predicted that, for all rotational states investigated, HeH^+ would be preferred over HeD^+ in the forward direction and HeD^+ would be preferred in the backward direction. The integral reaction cross section values for HeH^+ formation follow the trend $j = 0 > j = 1 > j = 2 > j = 3$ up to $E_{trans} = 0.9$ eV. At higher energies, the trend becomes $j = 0 > j = 1 > j = 3 > j = 2$. For the HeD^+ channel, the integral reaction cross section values follow the trend $j = 0 \sim j = 2 > j = 3 > j = 1$. The total σ^R values are the largest for $j = 0$ and the smallest for $j = 1$ over the entire translational energy range. The computed σ^R values for $j = 0$ at $E_{trans} = 1.0$ eV are in near quantitative agreement with the experimental results (which were not $j = 0$ selected). The experimental Γ_σ value at $E_{trans} = 1.0$ eV is slightly less than the computed value for $j = 0$ and 3. The Γ_σ values are strongly dependent on j, in contrast to the marginal dependence shown by earlier QCT calculations.

Acknowledgment. A.K.T. thanks the Council of Scientific and Industrial Research (CSIR), New Delhi, for a research fellowship. N.S. thanks the Department of Science and Technology, New Delhi, for a JC Bose fellowship. This study was supported in part by a grant from CSIR, New Delhi.

References and Notes

(1) Maiti, B.; Sathyamurthy, N. *Proc. Indian Natl. Sci. Acad. A* **2000**, *66*, 59.
(2) Tang, X. N.; Xu, H.; Zhang, T.; Hou, Y.; Chang, C.; Ng, C. Y.; Chiu, Y.; Dressler, R. A.; Levandier, D. J. *J. Chem. Phys.* **2005**, *200122*, 164301.
(3) Klein, S.; Friedman, L. *J. Chem. Phys.* **1964**, *41*, 1789.
(4) Turner, T.; Dutuit, O.; Lee, Y. T. *J. Chem. Phys.* **1984**, *81*, 3475.
(5) Bhalla, K. C.; Sathyamurthy, N. *Chem. Phys. Lett.* **1989**, *160*, 437.
(6) Joseph, T.; Sathyamurthy, N. *J. Chem. Phys.* **1984**, *80*, 5332.
(7) Kumar, S.; Sathyamurthy, N.; Bhalla, K. C. *J. Chem. Phys.* **1993**, *98*, 4680.
(8) Kalyanaraman, C.; Clary, D. C.; Sathyamurthy, N. *J. Chem. Phys.* **1999**, *111*, 10910.
(9) Tiwari, A. K.; Panda, A. N.; Sathyamurthy, N. *J. Phys. Chem. A* **2006**, *110*, 395.
(10) Palmieri, P.; Puzzarini, C.; Aquilanti, V.; Capecchi, G.; Cavalli, S.; Fazio, D. De; Aguilar, A.; Gimenez, X.; Lucas, J. M. *Mol. Phys.* **2000**, *98*, 1835.
(11) Balakrishnan, N.; Kalyanaraman, C.; Sathyamurthy, N. *Phys. Rep.* **1997**, *280*, 79.
(12) Zhang, J. Z. H. *Theory and Applications of Quantum Molecular Dynamics*; World Scientific: Singapore, 1999.

(13) Gögtas, F.; Balint-Kurti, G. G.; Offer, A. R. *J. Chem. Phys.* **1996**, *104*, 7927.
(14) Marston, C. C.; Balint-Kurti, G. G. *J. Chem. Phys.* **1989**, *91*, 3571.
(15) Feit, M. D.; Fleck, J. A., Jr.; Steiger, A. *J. Chem. Phys.* **1982**, *47*, 412.
(16) Kosloff, D.; Kosloff, R. *J. Comput. Phys.* **1983**, *52*, 35.
(17) Parker, G. A.; Light, J. C. *Chem. Phys. Lett.* **1982**, *89*, 483. Light, J. C.; Hamilton, I. P.; Lill, J. V. *J. Chem. Phys.* **1985**, *82*, 1400.
(18) Pack, R. T *J. Chem. Phys.* **1974**, *60*, 633.
(19) Maiti, B.; Kalyanaraman, C.; Panda, A. N.; Sathyamurthy, N. *J. Chem. Phys.* **2002**, *117*, 9719.
(20) Tiwari, A. K.; Sathyamurthy, N. *Chem. Phys. Lett.* **2005**, *414*, 509.
(21) Aquilanti, V.; Capecchi, G.; Cavalli, S.; Fazio, D. De; Palmieri, P.; Puzzarini, C.; Aguilar, A.; Gimenez, X.; Lucas, J. M. *Chem. Phys. Lett.* **2000**, *318*, 619.